Food Measure (2017) 11:1003–1010
DOI 10.1007/s11694-017-9475-8

ORIGINAL PAPER

Freezing-induced proton dynamics in tofu evaluated by low-field nuclear magnetic resonance

Yong Li[1,2,3] · Wentao Shi[1,2,3] · Shasha Cheng[1,2,3] · Haitao Wang[1,2,3] · Mingqian Tan[1,2,3]

Received: 19 October 2016 / Accepted: 17 January 2017 / Published online: 2 March 2017

Abstract The main purpose of the study was to understand and interpret the effects of freezing times on the proton dynamics and chrominance of tofu. Low-field nuclear magnetic resonance (LF-NMR) and magnetic resonance imaging (MRI) were used to monitor real-time changes in microstructure and water distribution at different freezing times. The T_2 relaxation parameters included the relative intensity (A_{2i}) and the population of T_{2i} component (M_{2i}). Three proton populations focusing on approximately 0.93–4.72, 25–49, and 402–505 ms were identified as T_{2b}, T_{21}, and T_{22}, respectively. The generated ice crystals damaged the hydration layer of the soybean protein and T_{2b} increased over the 2 h. The side chains of the soybean protein then began to unite owing to the protein's reduced affinity for water, making the protons of the hydrophilic groups exchangeable, and resulting in decreased mobility of the T_{2b} fraction. The appearance of exchangeable hydrophilic group protons caused an increase in A_{2b} from 2 to 6 h. The subsequent increases in A_{2b} and M_{2b} 6 h later were due to access to the unfrozen free water. The water molecules (T_{21} fraction) changed into ice crystals, reducing A_{21} and M_{21}. The disappearance of the T_{22} fraction peak 6 h later was attributed to residual unfrozen water molecules, with the minor component turning into ice with a fast relaxation time. The MRI results showed that the outline of the sample was blurred at 2 h and could not be detected 6 h later. Significant correlations were further detected between T_2 relaxation parameters and color parameters. LF-NMR has great potential as a reliable tool for the study of tofu.

Keywords Frozen tofu · Freezing time · Low-field nuclear magnetic resonance · Magnetic resonance imaging

✉ Yong Li
liyong_dlpu@163.com

✉ Mingqian Tan
2468750030@qq.com

[1] School of Food Science and Technology, National Engineering Research Center of Seafood, Dalian Polytechnic University, Qinggongyuan 1, Ganjingzi District, Dalian 116034, China

[2] Engineering Research Center of Seafood of Ministry of Education of China, Dalian 116034, China

[3] Liaoning Key Laboratory of Food Biological Technology, Dalian 116034, China

Introduction

Tofu, or soybean curd, is a traditional Chinese soya products; it is a gel-like food that is made by adding various coagulants to soymilk [1]. Fresh tofu contains innumerable holes of various sizes. Some holes are connected to each other and some are closed forming small containers, both are both filled with water. At atmospheric pressure, the water inside tofu changes into ice when the temperature falls below 0 °C. The volume of the tofu simultaneously increases by approximately 10%. Ice at atmospheric pressure—denoted as ice I (density, 0.92 g/cm^3)—is the only ice that is less dense than liquid water [2]. In other words, only ice I expands in volume during phase transition; high-pressure ices (ice II–ice IX) do not [3]. When ice I expands the original pores are stretched and the whole piece of tofu is extended to form a mesh. When the ice melts and flows out of the tofu, it leaves a honeycomb structure comprising a great many holes, which gives the tofu a gray appearance. Compared with fresh tofu, frozen tofu has a disrupted structure and a spongy texture, especially when it is slowly frozen at −20 °C and atmospheric pressure [2]. It is just a disrupted and porous texture that makes frozen tofu layered

on the palate and tasty. Moreover, frozen tofu is rich in dietary fiber, which promotes the metabolism of fat, and its loose and porous structure facilitates fat absorption.

There have been many studies on frozen tofu in recent years: Chuang et al. [4] studied the effects of cryoprotectants on the textural changes in tofu during the frozen stage; Frozen wild blueberry tofu soymilk desserts were obtained by Camire et al. [5]; Fuchigami et al. [2] studied the effects of high-pressure thawing on the structural and textural quality of high-pressure frozen tofu; Fuchigami et al. [6] researched the effects of trehalose and hydrostatic pressure on the structure and sensory properties of frozen tofu; and the effects of freezing soybeans on the quality of tofu were investigated by Noh et al. [7]. These studies have focused on the texture, structure, and sensory evaluation of frozen tofu. However, the effects of freezing time on proton dynamics in frozen tofu have not yet been reported.

Foods mainly comprise water and large molecules, which suggests that proton relaxation reflects the physicochemical properties of individual compounds and the interaction between water and large molecules. Because spin–spin relaxation (T_2) has a greater effect on relaxation time in a multi-phase environment than spin–lattice relaxation (T_1) [8], T_2 is often used as an indicator to monitor the dynamic state of water in protein gel systems [9]. T_2 depends on the microenvironment of the proton, and is closely related to the binding force and the degree of freedom of protons [10]. T_1 and T_2 are both determined by low-field nuclear magnetic resonance (LF-NMR), which is a rapid and nondestructive technique. The protein gel structure of tofu has been studied using LF-NMR. Li et al. [11, 12] used LF-NMR to investigate the effects of high-pressure homogenization on water distribution in tofu using T_2 measurements, and succeeded in applying T_2 relaxation measurements to determine the water holding capacity of tofu. LF-NMR has also proved to be a powerful tool in the study of other food including cake [13], bread [14], vegetables [15–18], cheese [19], chocolate [20], hake [21] and pasta [22]. Another kind of NMR technology, magnetic resonance imaging (MRI) is often used in medicine to investigate the structural abnormalities of the body [23], but it is also considered an accurate and nondestructive method of visualizing the internal structure of food [24]. Moreover, the combination of NMR and MRI has emerged as a means of investigating food processing [25, 26]. In particular, water mobility and distribution in biological macromolecular systems have been monitored using both NMR and MRI [27, 28], and NMR has also been used to investigate ice relaxation behavior in frozen sucrose–protein solutions [29].

The studies mentioned above suggest that NMR and MRI might be useful for exploring the preparation of frozen tofu. Therefore, in the present work, we used LF-NMR to investigate the effects of freezing time on the proton dynamics of frozen tofu using T_2 relaxation and MRI. We used NMR and MRI to investigate the mobility, distribution and structural changes of water within frozen tofu during freezing. Herein, we also discuss the relationship between changes in the color of frozen tofu and freezing time; the relationships between the individual T_2 relaxation parameters and the color of tofu during freezing were investigated using NMR.

Experimental

Samples preparation

Commercial soybeans from northeast China were kindly provided by the Key Laboratory of Biology and Genetic Improvement of Soybeans, the Ministry of Agriculture, People's Republic of China (Nanjing, People's Republic of China). The soybeans were rinsed and soaked in deionized water at a ratio of 1:5 (w/w) for 15 h at ambient temperature. They were then homogenized using a DJ12B-K5 household soymilk maker (Joyoung Co., Ltd., Shandong, China), heated gradually to 98 °C, and maintained at 98 °C for 6 min. When the soymilk maker cycle was complete, the soymilk was filtered twice through double layers of cheesecloth.

The soymilk (2 L) was boiled using a JYC-21HEC05 electromagnetic oven (Joyoung Co., Ltd., Shandong, China), stirred for 3 min, and cooled to 90 °C. Coagulants (magnesium chloride and glucono-delta lactone; w/w, 7:3) were dispersed at a concentration of 3% (w/w) in deionized water at 90 °C. The soymilk was immediately added to the coagulant solution at room temperature and continuously stirred with a stainless steel spoon for 10 s. The mixture was then decanted into a water bath for 20 min at 90 °C, then transferred to a wooden mold and pressed at 0.01 kg/cm^2 for 30 min to produce the tofu curd. The curd was stored at 4 °C in a refrigerator before analysis.

NMR relaxometry

NMR relaxometry experiments were performed on a MesoMR23-060V-I NMR Analyzer (Niumag Co., Ltd., Shanghai, China) equipped with a 0.5 T permanent magnet, operated at 23.2 MHz for 1H-resonance frequency and 32 °C; a temperature control system, was used to maintain the temperature of the samples (− 20 to 130 °C). After storage at 4 °C for 24 h, the tofu samples were cut into small pieces of approximately 7 g. The tofu samples obtained from the middle of the tofu curds were frozen at −20 °C in a DW-25L262 refrigerator (Haier Specialty Electrical Appliance Co., Ltd., Shandong, China) for 0, 0.25, 0.5, 1, 2, 4, 6, 8,

12 and 24 h. Each tofu sample corresponding to a particular freezing time-points was placed in a glass NMR tube. The glass tube was inserted into a 40-mm diameter radio frequency coil to measure T_2 relaxation times, using the Carr–Purcell–Meiboom–Gill (CPMG) sequence with a τ value of 300 μs (intervals between the 90° and 180° and the 90° and 180° pulses of 20 and 41 μs, respectively). The tofu samples were maintained at −20 °C. Each measurement of 8 scans was performed with 6000 echoes to prevent imperfect pulse settings. The repetition time between subsequent scans was 2 s and each measurement was performed in triplicate. MultiExp Inv- analysis software (Niumag Electric Corporation, Shanghai, China) was used to obtain distributed multi-exponential fitting curves, namely LF-NMR relaxation curves, using the inverse Laplace transform algorithm. The relaxation time (T_{2i}), its corresponding relative intensity (A_{2i}), and the water population (area ratio; M_{2i}) were calculated using the LF-NMR relaxation curves. Each sample was evaluated ten times and each test was completed with five samples at the various freezing time-points.

MRI

MRI data were also acquired on the MesoMR23-060V-I NMR Analyzer. Proton density weighted images were acquired by spin echo sequence. The echo time (TE) was 20 ms and the repetition time (TR) was 1600 ms. Four coronal slices were acquired; each was 2 mm thick and the interval between slices was 2 mm. The 3rd slice was used for data analysis. The field of view (FOV) was 100 mm × 100 mm. The image files were analyzed using OsiriX 7.5.1 (Pixmeo, Bernex, Geneva, Switzerland).

Color

The color of the tofu samples was evaluated at the various freezing time-points using a HunterLab UltraScan PRO colorimeter (HunterLab Co., Ltd., USA). A standard white tile with reflectance values of L = 90.2, a = 0.4, and b = 3.4 was used as a reference. A representative sample was placed on a 3-cm petri dish. Hunter L (0.00 = dark black, 100.00 = white), a (+ = red, − = green), and b (+ = yellow, − = blue) were then determined for each sample. Whiteness values were calculated using the following equation:

$$H = 100 - [(100 - L)^2 + a^2 + b^2]^{1/2}$$

Color measurements were performed on five samples per batch.

Statistical analysis

Statistical analyses were carried out using SPSS version 18.0 (SPSS Inc., Chicago, IL, USA). One-factor analysis of variance (ANOVA) was carried out to evaluate the difference between means for each of the parameters. Statistical significance was set at (*) $p < 0.05$. Linear regression analysis was carried out using Origin 8.5.1 (Microcal, Northampton, Massachusetts, USA).

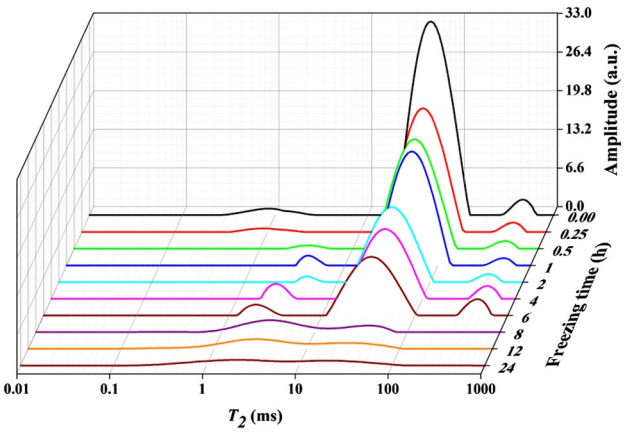

Fig. 1 LF-NMR T_2 multi-component inversion relaxation curves of tofu at different freezing times

Table 1 T_2 relaxation times (T_{2b}, T_{21}, T_{22}) of tofu at different freezing times

Freezing time (h)	T_{2b} (ms)	T_{21} (ms)	T_{22} (ms)
0	0.93 ± 0.07^{a}	47.76 ± 3.31^{cd}	450.30 ± 12.91^{ab}
0.25	1.07 ± 0.27^{a}	47.69 ± 0.00^{cd}	439.76 ± 0.00^{ab}
0.5	3.50 ± 0.38^{cd}	48.83 ± 1.98^{d}	439.76 ± 0.00^{ab}
1	4.01 ± 0.16^{d}	49.97 ± 1.98^{d}	472.13 ± 32.76^{bc}
2	4.72 ± 0.19^{e}	37.98 ± 3.95^{bc}	402.37 ± 41.90^{a}
4	2.78 ± 0.35^{bc}	38.78 ± 2.69^{bc}	505.26 ± 0.00^{c}
6	2.10 ± 0.15^{b}	34.62 ± 3.73^{ab}	493.97 ± 19.57^{bc}
8	3.85 ± 0.57^{d}	34.68 ± 9.51^{ab}	
12	3.28 ± 0.55^{cd}	30.28 ± 5.06^{ab}	
24	2.26 ± 0.65^{b}	25.20 ± 4.31^{a}	

Results are presented as the mean ± standard deviation. Means with different superscript letters within the same column are significantly different ($p < 0.05$)

Results and discussion

T_2 relaxation analysis

As shown in Fig. 1 and Table 1, the LF-NMR T_2 distribution and relaxation times were obtained for the tofu curds at different freezing times after multi-exponential fitting. The T_2 relaxation signals in tofu were mainly attributed to hydrogen protons in oil and water. According to Li's report [12], the T_2 relaxation time of the oil protons

Table 2 The relative intensity (A_{2b}, A_{21}, A_{22}) of T_2 components of tofu at different freezing times

Freezing time (h)	A_{2b}	A_{21}	A_{22}
0	18.21 ± 0.66^{b}	521.82 ± 15.73^{e}	17.70 ± 1.51^{a}
0.25	7.66 ± 2.81^{a}	340.63 ± 8.28^{d}	10.90 ± 0.68^{a}
0.5	6.31 ± 0.73^{a}	326.13 ± 1.86^{d}	10.35 ± 0.39^{a}
1	10.31 ± 0.59^{a}	315.63 ± 4.51^{d}	9.51 ± 1.17^{a}
2	5.86 ± 2.63^{a}	227.04 ± 15.69^{c}	11.32 ± 1.63^{a}
4	20.98 ± 1.04^{b}	202.15 ± 10.48^{b}	24.39 ± 7.91^{b}
6	17.23 ± 2.28^{b}	177.66 ± 37.18^{b}	25.47 ± 4.47^{b}
8	55.66 ± 6.35^{e}	19.71 ± 2.75^{a}	
12	51.52 ± 6.53^{e}	22.30 ± 2.40^{a}	
24	43.45 ± 4.18^{c}	24.68 ± 4.78^{a}	

Results are presented as the mean ± standard deviation. Means with different superscript letters within the same column are significantly different ($p < 0.05$)

in tofu obtained by vacuum freeze drying, centered at approximately 86–100 ms, accounted for less than 1% of the total T_2 relaxation proportions in tofu without vacuum freeze drying treatment. Consequently, the effect on T_2 relaxation measurements of the oil in tofu in this experiment was ignored in the following analysis of the results. Figure 1 indicates that tofu produced three peaks identified as T_{2b}, T_{21}, and T_{22} according to previous assignments [30, 31] after less than 6 h of freezing, and the number of peaks was the same as the number detected in Li's study [11]. When the freezing time was extended to 8 h, the number of peaks was reduced to two. The relaxation time of T_{2b} as the fastest fraction (0.93–4.72 ms) initially increased and then decreased with increasing freezing time. T_{21} was the intermediate fraction (25–49 ms) and its relaxation time presented a downtrend with increasing freezing time. In contrast, T_{22} was regarded as the slowest fraction (402–505 ms), and there were no regular changes in its relaxation time with increasing freezing time. The two components T_{2b} (0.93–4.72 ms) and T_{21} (25–49 ms) in the samples were similar to T_{2b} (1.5–2.5 ms) and T_{21} (21–49 ms) [11]. Moreover, the T_{2b} fraction (0.93–4.72 ms) was attributed to the water molecules tightly associated with the protein biopolymer. The T_{21} fraction (25–49 ms) was ascribed to the water molecules in the small meshes of the tofu microstructure. However, the third component T_{22} (402–505 ms) was markedly different to T_{22} (151–505 ms) [11]. The T_{22} fraction (402–505 ms) was attributed to the water molecules in the large pores and gaps in the three-dimensional tofu network. The difference in preparation of tofu between our research and Li's research [11] made a difference to the three-dimensional network of the tofu, leading to the difference in relaxation time of the T_{22} fraction.

The relative intensities (A_{2b}, A_{21}, and A_{22}) of the T_2 components are shown in Table 2. When the freezing time of tofu exceeded both 2 and 6 h, A_{2b} increased significantly. A_{21} decreased by degrees over the initial 6 h of freezing, and fell off significantly later ($p < 0.05$). A_{22} initially decreased and then increased with increasing freezing time. Table 3 shows the population (M_{2b}, M_{21}, and M_{22}) changes in the T_2 components with freezing time. T_{2b} accounted for only 2–8% of the total signal during the first 6 h of freezing time, and approximately 70% 8 h later. Moreover, T_{21} was a major component and occupied 80–95% of the total signal over the first 6 h, and approximately 25–36% after 8 h. The population of T_{22} significantly increased when the freezing time was prolonged to 4 h ($p < 0.05$). However, the T_{22} component remained a minor fraction throughout, and varied from 3 to 12% during 24 h of freezing.

Hills et al. [32] proposed that proton relaxation behavior not only reflects the state of water but also the state of biopolymers and morphology. Li et al. [11] assigned the three water fractions based on the microstructures of tofu. Tofu is a soybean protein matrix that is induced by coagulants, and it has a three-dimensional network structure composed of pores and meshes of various sizes. When tofu is subjected to freeze treatment, these pores and meshes form a more heterogeneous microenvironment. Furthermore, the formation of ice crystals and the freezing denaturation of the soybean protein also promote a more complex and diverse relaxation behavior in the water. When tofu begins to freeze, the water molecules (T_{21}) that maintain an intermediate distance from the surrounding protein network in the small meshes initially form into ice crystals and are precipitated out. Acids and salts in the small meshes form a concentrated solution in the residual water, leading to the denaturation

Table 3 T_2 populations (M_{2b}, M_{21}, M_{22}) of tofu at different freezing times

Freezing time (h)	M_{2b}	M_{21}	M_{22}
0	0.03 ± 0.00^{a}	0.94 ± 0.00^{a}	0.03 ± 0.00^{a}
0.25	0.02 ± 0.01^{a}	0.95 ± 0.00^{a}	0.03 ± 0.00^{a}
0.5	0.02 ± 0.00^{a}	0.95 ± 0.00^{a}	0.03 ± 0.00^{a}
1	0.03 ± 0.00^{a}	0.94 ± 0.00^{a}	0.03 ± 0.00^{a}
2	0.02 ± 0.01^{a}	0.93 ± 0.00^{a}	0.05 ± 0.01^{a}
4	0.08 ± 0.00^{a}	0.82 ± 0.03^{c}	0.10 ± 0.03^{b}
6	0.08 ± 0.00^{a}	0.80 ± 0.05^{c}	0.12 ± 0.04^{b}
8	0.71 ± 0.05^{c}	0.29 ± 0.04^{a}	
12	0.70 ± 0.05^{c}	0.30 ± 0.04^{a}	
24	0.64 ± 0.06^{b}	0.36 ± 0.06^{b}	

Results are presented as the mean ± standard deviation. Means with different superscript letters within the same column are significantly different ($p < 0.05$)

of soybean protein accompanied by salting-out effect. It was inferred that the greatest distance between the water molecules (T_{22}) in the large pores and the gaps in the surrounding protein network resulted in slower heat exchange than in the T_{21} fraction. Therefore, T_{21}, A_{21}, and M_{21} reflected the same decreasing tendency, and T_{22} changed irregularly. The significant increase in A_{22} and M_{22} after 4 h of freezing may have been caused by the excess of unfrozen free water in the small meshes. The disappearance of the T_{22} fraction peak 6 h later was attributed to the residual unfrozen water molecules, with the minor component turning into ice with a fast relaxation time. The soybean protein was slowly concentrated as the free water slowly froze. The advanced structure of protein is maintained by intramolecular hydrophobic bonds between non-polar groups, and by hydrogen bonds, the distribution of which is closely related to the structure and state of the molecules in the surrounding of protein [33, 34]. The hydration layer of the protein, namely water molecules (T_{2b}) tightly associated with the protein biopolymer, is damaged by the generation of ice crystals. The binding force between the T_{2b} fraction and the protein is weakened and T_{2b} increases during the first 2 h. Moreover, part of the T_{2b} fraction existing in the side chains of the soybean protein is frozen during the extension of freezing, which destroys the colloidal properties of the protein and reduces its affinity for water. Consequently, the side chains are united together and the protons of the hydrophilic groups became exchangeable [35]. Therefore, the decrease in the protein's affinity for water accompanied by exchangeable protons may be responsible for the change of T_{2b} during 2 to 24 h of freezing. The sudden increase of M_{2b} and the decrease of M_{21} at 8 h may be caused by the large difference in the freezing rate between T_{2b} and T_{21} with distinctively different states of water. The significant decrease of M_{2b} and the increase of M_{21} at 24 h require further study ($p < 0.05$).

When the samples are considered to be an integral component, the relaxation time (T_{2W}) and amplitude of the mono-component can be acquired after multi-exponential fitting, as seen in Fig. 2. The food matrix comprises water and large molecules, and the interaction between water and macromolecules is therefore the most important factor influencing the relaxation of hydrogen protons in the food matrix. As can be seen in Fig. 2, the relaxation time and amplitude both decreased with increasing freezing time. This phenomenon may be explained by the formation of ice crystals during the freezing process. Proton relaxation in ice crystals is too rapid to be detected by LF-NMR. To sum up, T_2 relaxation can be used to monitor the distribution of unfrozen water, and is considered a good indicator of the time-induced structural changes in tofu during freezing.

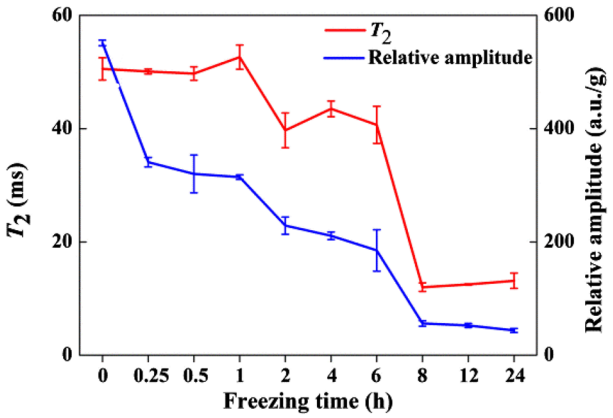

Fig. 2 LF-NMR T_2 mono-component inversion relaxation time and relative amplitude of tofu at different freezing times

MRI

MRI as a rapid and nondestructive method that can be used to detect the water distribution in the food matrix and to visualize the internal structural changes during processing. Figure 3A shows the pseudo-color images (low–high proton density, blue–red color) of the proton density-weighted images (PDWIs) of tofu at different freezing time-points. The PDWIs illustrate the total water distribution including that of bound water and free water. The differences in the layers in each sample at different freezing times were observed intuitively. Specifically, the right edge of the sample emitted a much lower signal intensity (blue color) than other parts owing to the low water content. Moreover, the low signal from the area of the right edge progressively increased. This may have resulted from immediate contact with the fridge drawer and the rapid formation of ice crystals. When the freezing time was increased to 2 h, the outline of the sample became blurred with the increasing number of ice crystals. Moreover, when the sample was subjected to 6 h of freezing, the outline could not be determined by MRI. The result was in accordance with the sharp decrease in the relative intensity of T_2 components at 6 h of freezing time, as shown in Table 2. It is possible to infer that there were few ice crystals before 1 h of freezing; subsequently, a large number of ice crystals were generated up to 2 h, and the number remained stable after 6 h. The relative intensity of the PDWIs is shown in Fig. 3B. It was obvious that the intensity of the PDWIs decreased after freezing, which was consistent with the relative intensity of the T_2 components. These results reveal that tofu requires at least 6 h of freezing.

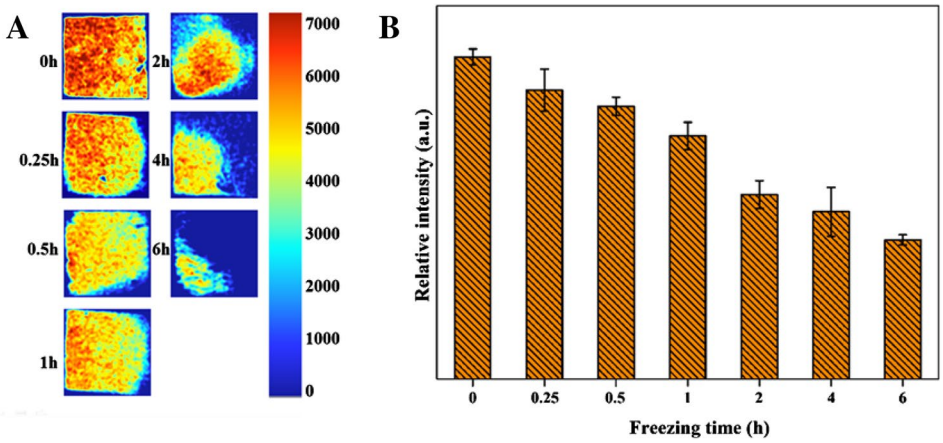

Fig. 3 PDWIs of (**A**) and the corresponding histogram of relative intensity of PDWIs of (**B**) of tofu at different freezing times

Relationship between chrominance and LF-NMR

NMR is a rapid and nondestructive analytical method that can be used instead of time-consuming and sample-destructive analytical methods. Moreover, there is a strong correlation between NMR parameters and relative physico-chemical parameters. Color is a key parameter in tofu quality. Good-quality tofu is white or light yellow. Therefore, we investigated the correlation between the NMR parameters and the color parameters of tofu at various freezing time-points in this study. The tofu sample was tested using a Hunter colorimeter as shown in Table 4. We found that the L and whiteness values decreased with increasing freezing time ($p < 0.05$). The major cause of this phenomenon was the interactions between the soybean protein and water, which deteriorates with increasing freezing time, resulting in enhanced of protein–protein interactions and the precipitation of soybean protein. The destruction of the three-dimensional network structure of cryopreserved tofu affects the reflection of light, and reduces the L and whiteness values of the tofu sample. In this study, the L and whiteness values did not significantly decrease after the first 1 h, which indicates that the three-dimensional network structure was not obviously damaged during the primary freezing stage. Moreover, the a and b values changed little change during the freezing time, which indicates that the physico-chemical changes to the components in tofu resulting from the freezing process did not affect the absorption wavelength. Hence, the a and b as chromaticity index values changed little.

In a previous study, Li et al. [12] discovered that there is a strong linear relationship between the T_{2i} relaxation time and the water-holding capacity of tofu. Therefore, the linear relationships between the NMR parameters and the color parameters of tofu during the freezing process are of particular interest (Table 5). In our study, there was a strong linear relationship between the L values and the NMR parameters ($0.655 \le R^2 \le 0.942$), which was significant except in the case of T_{2b}. As similar correlation of values ($0.676 \le R^2 \le 0.927$) was observed for whiteness, but there was no significant correlation in the case of T_{2b}. For a and b values, significant correlation was restricted to T_{22}, A_{22},

Table 4 Hunter L, a, b and whiteness value of tofu at different freezing times

Freezing time (h)	L*	a*	b*	H
0	88.89 ± 0.36^{e}	0.13 ± 0.16^{b}	18.70 ± 0.63^{abc}	78.24 ± 0.65^{e}
0.25	89.28 ± 0.24^{e}	0.34 ± 0.06^{b}	17.21 ± 0.23^{ab}	79.61 ± 0.15^{e}
0.5	88.67 ± 0.14^{e}	0.46 ± 0.08^{b}	17.18 ± 0.18^{ab}	79.41 ± 0.17^{e}
1	89.08 ± 0.42^{e}	0.25 ± 0.14^{b}	18.16 ± 0.19^{abc}	78.81 ± 0.37^{e}
2	82.42 ± 0.49^{d}	0.61 ± 0.15^{b}	21.03 ± 0.76^{c}	72.58 ± 0.78^{d}
4	77.15 ± 3.13^{c}	0.26 ± 0.36^{b}	19.47 ± 0.83^{bc}	69.91 ± 2.48^{c}
6	76.60 ± 1.49^{c}	0.30 ± 0.50^{b}	20.86 ± 0.62^{c}	68.64 ± 1.38^{c}
8	56.69 ± 3.11^{b}	-0.70 ± 0.36^{a}	15.73 ± 3.74^{a}	53.74 ± 1.83^{b}
12	53.02 ± 3.53^{a}	1.47 ± 0.55^{c}	16.01 ± 1.95^{a}	50.29 ± 3.05^{a}
24	51.48 ± 3.32^{a}	1.66 ± 0.39^{c}	16.82 ± 2.65^{ab}	48.53 ± 2.42^{a}

Results are presented as the mean ± standard deviation. Means with different superscript letters within the same column are significantly different ($p < 0.05$)

Table 5 Linear regression analysis between NMR parameters and Hunter values and whiteness

T_2 parameters	R	R^2	p
Correlation with L*			
T_{2b}	0.154	0.024	ns
T_{21}	0.810	0.655	$p < 0.01$
T_{22}	0.460	0.212	$p < 0.05$
A_{2b}	0.930	0.865	$p < 0.01$
A_{21}	0.899	0.809	$p < 0.01$
A_{22}	0.811	0.657	$p < 0.01$
M_{2b}	0.958	0.918	$p < 0.01$
M_{21}	0.971	0.942	$p < 0.01$
M_{22}	0.869	0.755	$p < 0.01$
Correlation with a*			
T_{2b}	0.024	0.001	ns
T_{21}	0.508	0.259	$p < 0.05$
T_{22}	0.246	0.061	ns
A_{2b}	0.283	0.080	ns
A_{21}	0.387	0.150	$p < 0.1$
A_{22}	0.194	0.038	ns
M_{2b}	0.387	0.150	$p < 0.1$
M_{21}	0.347	0.120	$p < 0.1$
M_{22}	0.094	0.009	ns
Correlation with b*			
T_{2b}	0.111	0.012	ns
T_{21}	0.040	0.002	ns
T_{22}	0.161	0.026	ns
A_{2b}	0.581	0.337	$p < 0.05$
A_{21}	0.286	0.082	ns
A_{22}	0.583	0.340	ns
M_{2b}	0.584	0.341	$p < 0.05$
M_{21}	0.547	0.299	$p < 0.05$
M_{22}	0.645	0.416	$p < 0.05$
Correlation with H			
T_{2b}	0.152	0.023	ns
T_{21}	0.822	0.676	$p < 0.01$
T_{22}	0.417	0.174	$p < 0.1$
A_{2b}	0.921	0.848	$p < 0.01$
A_{21}	0.896	0.802	$p < 0.01$
A_{22}	0.800	0.640	$p < 0.01$
M_{2b}	0.951	0.904	$p < 0.01$
M_{21}	0.963	0.927	$p < 0.01$
M_{22}	0.852	0.727	$p < 0.01$

M_{2b}, and M_{22} and A_{2b}, M_{2b}, M_{22}, and M_{23}, respectively. The correlation between the values suggests the potential use of NMR parameters in monitoring the color change of tofu at different freezing time-points.

Conclusions

In this study we proved that the investigation of the tofu freezing process at atmospheric pressure is feasible using LF-NMR and MRI. The freezing process changed free water (T_{21} and T_{22} fractions) into ice crystals. However, the distances to the surrounding protein network were different in these two water fractions, and consequently their heat exchange rates and ice crystal generation rates were different. This explains why the T_{21} and T_{22} parameters behaved differently during the freezing process. The freezing denaturation of the soybean protein weakened its affinity for water, and the T_{2b} protons became more active. Furthermore, the union of the side chains of the soybean protein produced exchangeable protons on the hydrophilic groups, which decreased the relaxation time of the T_{2b} protons and increased the A_{2b} from 2 to 6 h. In the residual frozen water, access to the T_{2b} fraction was accompanied by an increase in A_{2b} and M_{2b} after 6 h of freezing. The water proton migration and the formation of ice crystals destroyed the three-dimensional network structure and changed the tofu population distribution, resulting in a decrease in the L and whiteness values. Therefore, there was significant linear correlation between the T_2 parameters and the Hunter colorimetric readings. To sum up, LF-NMR and MRI can be used for rapidly determining the state of water and for visualizing the water distribution in tofu during freezing.

Acknowledgements The authors are grateful for the precious comments and careful corrections made by the anonymous reviewers. The authors would also like to acknowledge the Scientific Research Foundation for the Doctors (61020712).

Compliance with Ethical Standards

Conflict of interest The authors declare that there is no conflict of interest.

References

1. V.A. Obatolu, Eur. Food. Res. Technol. **226**, 467–472 (2008)
2. M. Fuchigami, A. Teramoto, N. Ogawa, J. Food Sci. **63**, 1054–1057 (1998)
3. Schulson E. M, Duval P, Schulson E. M, Duval. P. *Physical Properties: Elasticity, Friction and diffusivity creep and Fracture of Ice* (Cambridge University Press, New York, 2009)
4. S.H. Chung, W.S. Choi, H.S. Son, C.H. Lee, Korean J. Food. Sci. Technol. **31**, 957–963 (1999)
5. M.E. Camire, M.P. Dougherty, Y.-H. Teh, J. Food Sci. **71**, S119–S123 (2006)
6. M. Fuchigami, N. Ogawa, A. Teramoto, Innov. Food Sci. Emerg. **3**, 139–147 (2002)

7. E.J. Noh, S.Y. Park, J.I. Pak, S.T. Hong, S.E. Yun, Food Chem. **91**, 715–721 (2005)
8. G.R. Trout, Meat Sci. **23**, 235–252 (1988)
9. C.-I. Cheigh, H.-W. Wee, M.-S. Chung, Food Res. Int. **44**, 1102–1107 (2011)
10. H.C. Bertram, H.J. Andersen, A.H. Karlsson, Meat Sci. **57**, 125–132 (2001)
11. T. Li, X. Rui, K. Wang, M. Jiang, X. Chen, W. Li, M. Dong, Innov. Food Sci. Emerg. **30**, 61–68 (2015)
12. T. Li, X. Rui, W. Li, X. Chen, M. Jiang, M. Dong, J. Agric. Food Chem. **62**, 8594–8601 (2014)
13. A. Luyts, E. Wilderjans, I. Van Haesendonck, K. Brijs, C.M. Courtin, J.A. Delcour, Food Chem. **141**, 3960–3966 (2013)
14. L. Manzocco, S. Calligaris, S. Da Pieve, S. Marzona, M.C. Nicoli, Food Res. Int. **49**, 778–782 (2012)
15. M. Koizumi, S. Naito, T. Haishi, S. Utsuzawa, N. Ishida, H. Kano, Magn. Reson. Imaging. **24**, 1111–1119 (2006)
16. K.L. McCarthy, M.J. McCarthy, V. Rakesh, A.K. Datta, J. Food Sci. **75**, E66–E72 (2010)
17. L. Zhang, D.M. Barrett, M.J. McCarthy, J. Food Sci. **78**, E50–E55 (2013)
18. G. Adiletta, G. Iannone, P. Russo, G. Patimo, S. De Pasquale, M. Di Matteo, Int. J. Food Sci. Technol. **49**, 2602–2609 (2014)
19. M. Musse, S. Challois, D. Huc, S. Quellec, F. Mariette, J. Food Eng. **121**, 152–158 (2014)
20. M.E. Miquel, L.D. Hall, Food Res. Int. **35**, 993–998 (2002)
21. I. Sanchezalonso, I. Martinez, J. Sanchezvalencia, M. Careche, Food Chem. **135**, 1626 (2012)
22. G. Pasini, F. Greco, M. Cremonini, A. Brandolini, R. Consonni, M. Gussoni, J. Agric. Food Chem. **63**, 5072 (2015)
23. S. Nakano, J. Kousaka, K. Fujii, K. Yorozuya, M. Yoshida, Y. Mouri, M. Akizuki, R. Tetsuka, T. Ando, T. Fukutomi, Y. Oshima, J. Kimura, T. Ishiguchi, O. Arai, Breast Cancer Res. Treat. **134**, 1179–1188 (2012)
24. G. Guthausen. TrAC Trends in Analytical Chemistry
25. S. Geng, H. Wang, X. Wang, X. Ma, S. Xiao, J. Wang, M. Tan, Anal. Methods. **7**, 2413–2419 (2015)
26. F. Mariette, Curr. Opin. Colloid Interface Sci. **14**, 203–211 (2009)
27. J. Liu, K. Zhu, T. Ye, S. Wan, Y. Wang, D. Wang, B. Li, C. Wang, Food Res. Int. **51**, 437–443 (2013)
28. C. Mcdonnell, P. Allen, E. Duggan, J.M. Arimi, E. Casey, G. Duane, J.G. Lyng, Meat Sci. **95**, 51–58 (2013)
29. T. Lucas, F. Mariette, S. Dominiawsyk, D.L. Ray, Food Chem. **84**, 77–89 (2004)
30. H.C. Bertram, S. Dønstrup, A.H. Karlsson, H.J. Andersen, Meat Sci. **60**, 279–285 (2002)
31. H.C. Bertram, H.J. Andersen, A.H. Karlsson, Meat Sci. **57**, 125 (2001)
32. B.P. Hills, S.F. Takacs, P.S. Belton, Food Chem. **37**, 95–111 (1990)
33. K. Hashizume, K. Kakiuchi, E. Koyama, T. Watanabe, Agric. Biol. Chem. **35**, 449–459 (1971)
34. S. Benjakul, W. Visessanguan, C. Thongkaew, M. Tanaka, Food Res. Int. **36**, 787–795 (2003)
35. M.I. Marques, J.M. Borreguero, H.E. Stanley, N.V. Dokholyan, Phys. Rev. Lett. **91**, 138103 (2002)